Pergamon

Cement and Concrete Research 30 (2000) 775–779

CEMENT AND CONCRETE RESEARCH

Microstructural identification of thaumasite in concrete by backscattered electron imaging at low vacuum

Renhe Yang*, Nick R. Buenfeld

Department of Civil and Environmental Engineering, Imperial College of Science, Technology and Medicine, Imperial College Road, London SW7 2BU, UK

Received 6 August 1999; accepted 22 February 2000

Abstract

A few cases of sulfate attack, involving the formation of thaumasite, have been discovered in site concrete. A technique able to detect small amounts of thaumasite in the presence of ettringite is necessary for developing a detailed understanding of the mechanism of thaumasite sulfate attack and for assessing concrete structures exposed to sulfates. Optical microscopy and X-ray diffraction (XRD) analysis may be used to identify thaumasite in large quantities in a concrete sample. However, the usefulness of optical microscopy is limited by its resolution. When ettringite is abundant, the identification of thaumasite by XRD analysis is very difficult as the d-spacings between thaumasite and ettringite are so similar that the XRD peaks of thaumasite in small quantity may be overwhelmed by the adjacent strong peaks of ettringite. In this study, concrete specimens containing bands of both ettringite and thaumasite were examined by backscattered electron imaging, first under low vacuum (9 Pa) and then under high vacuum. Prior to examination, the specimens were dried at 50°C, resin impregnated, then polished. Under high vacuum, thaumasite and ettringite bands appeared heavily cracked and of similar gray scale; they could not be differentiated visually, only by X-ray microanalysis, which is laborious and sometimes imprecise. Under low vacuum, the appearance of ettringite was similar to that in high vacuum, but thaumasite was different, with very few cracks and darker gray scale. This suggests that thaumasite requires a higher vacuum than ettringite to lose its structural water. Thus, low vacuum SEM can be used to identify thaumasite and to differentiate between thaumasite and ettringite.

Keywords: SEM; Low vacuum; Thaumasite; Ettringite; Sulfate attack

1. Introduction

Sulfate attack of concrete, involving the formation of ettringite and gypsum, has been recognized for many years. However, only a few cases of sulfate attack involving the formation of thaumasite have been discovered in site concrete [1–6]. The mechanisms of the two forms of sulfate attack are different. One consequence is that sulfate-resisting Portland cement, which provides high resistance to conventional sulfate attack, is vulnerable to the thaumasite form of sulfate attack [5,6].

Ettringite is a normal product of cement hydration and the thaumasite form of sulfate attack always starts with the formation of small quantities of thaumasite which may gradually develop into large deposits. Therefore, a technique able to detect small amounts of thaumasite in the presence of ettringite is necessary for developing an understanding of the mechanism of thaumasite sulfate attack and for assessing the current condition and residual life of concrete structures exposed to sulfates.

Thaumasite ($CaSiO_3 \cdot CaCO_3 \cdot CaSO_4 \cdot 15H_2O$) belongs to the family of ettringite-type crystal hydration products. Its crystalline structure, X-ray diffraction (XRD) pattern, microstructural features and many of its optical properties are similar to those of ettringite ($3CaO \cdot Al_2O_3 \cdot 3CaSO_4 \cdot 32H_2O$). Such similarities create difficulties in differentiating thaumasite and ettringite. Optical microscopy [5,7] and XRD analysis [8] may be used to identify thaumasite in large quantities in a concrete sample. However, for the sample with thaumasite present at relatively low contents or concentrated in small areas, the usefulness of optical microscopy is limited by its resolution. The d-spacings of thaumasite (Powder diffraction file 25-127, JCPDS) and ettringite (Powder diffraction file 9-414, JCPDS) are sufficiently similar that the XRD peaks of thaumasite in small

* Corresponding author. Tel.: +44-171-594-5957; fax: +44-171-225-2716.

E-mail address: renhe.yang@ic.ac.uk (R. Yang).

0008-8846/00/$ – see front matter
PII: S0008-8846(00)00244-1

quantity may be overwhelmed by the adjacent strong peaks of ettringite. Consequently, the identification of thaumasite by XRD analysis is difficult and especially so at low thaumasite or high ettringite contents.

SEM with X-ray microanalysis has the potential to identify thaumasite, from massive down to trace amounts. However, thaumasite and ettringite have similar microstructural features in images obtained by SEM in the conventional high vacuum mode [5,7]. Hence, thaumasite identification in the SEM currently relies on X-ray microanalysis. Much experience and many analyses are required to judge whether the material being analyzed is thaumasite, sulfate-rich C-S-H gel [9] or a mixture of C-S-H gel and gypsum or ettringite.

In this study, SEM in the low vacuum mode was used to examine concrete containing both ettringite and thaumasite. It was discovered that SEM at low vacuum facilitates the identification of thaumasite even in very small amounts.

2. Experimental

The source of concrete was a 152 mm thick precast concrete tunnel lining that had been buried in London Clay for 30 years. The concrete was made of ordinary Portland cement, Thames Valley gravel (flint), and siliceous sand (quartz). The concrete mix proportions and cement composition are unknown. Cores, 100 mm diameter, 152 mm long were wet cut from the lining and then 40 × 20 × 5 mm specimen blocks were sliced from the surface of the concrete that had been in contact with the ground, using a diamond saw. The specimen blocks were dried in an oven at 50°C for 3 days and were then resin impregnated under vacuum at a pressure of the order of 10^{-3} Pa for a period of around 15 min. The impregnated specimens were lapped on a sand dish of 200 μm and polished on cloths saturated with diamond particles at four levels from 9 μm down to 1/4 μm. The polished specimens were stored in a CO_2-free cabinet at 55% RH, until required for the SEM observations at low vacuum.

Carbon coating was not required for the specimens to be observed at low vacuum. After the observations by SEM at low vacuum, the specimens were further dried for 2 days by vacuum pump at a pressure of the order of 10^{-4} Pa and they were then carbon coated under pressure down to around 7×10^{-5} Pa. The carbon-coated specimens were then re-examined by SEM, this time at high vacuum.

A JEOL 5410LV SEM was used. The pressure in the sample chamber could be adjusted in the range of 6–66 Pa. The instrumental parameters for SEM were: accelerating voltage = 20 kV; loaded beam current = 55 μA; beam spot size (SS) setting = 12; pressure in the specimen chamber, 9 Pa (low vacuum mode) or around 10^{-4} Pa (high vacuum mode). The quantitative X-ray microanalysis was carried out in the high vacuum mode. The accelerating voltage was maintained at 20 kV and the beam spot size setting was increased to 18. The ZAF procedure was used to quantify 11 elements (Na, Mg, Al, Si, P, S, K, Ca, Ti, Mn, and Fe). Oxygen was determined by stoichiometry.

Raman spectroscopic measurements were carried out using a Renishaw Raman Microprobe (system 2000), with a laser (488 nm) excitation source having a power at the specimen of the order of 4 mW. While the equipment is capable of spatial resolution of approximately 2 μm, for these analyses of a transparent phase, it appeared to be degraded to approximately 50 μm [10].

3. Results and discussion

Sulfate attack was diagnosed to be occurring to a depth of less than 5 mm into the concrete. Carbonation was commonly identified in the region suffering from sulfate attack. A backscattered electron (bse) image obtained by SEM at low vacuum is shown in Fig. 1; the fine ettringite bands are typical of conventional sulfate attack. The microstructural features of the ettringite bands appear to be very similar to those commonly observed by SEM in the conventional high vacuum mode [11]. In addition to the ettringite bands, visually different bands were also present in the same areas (Fig. 2a and b). The latter had a uniform gray level that was darker than the ettringite, C-S-H gel, and siliceous sand. Unlike the ettringite, there were very few cracks in these bands. The cracks observed in the ettringite bands were believed to be caused by shrinkage during drying. Some of the dark bands had apparently developed in parallel with the ettringite bands (Fig. 2b).

The same specimens were further vacuum dried, carbon coated and were then observed under SEM in the high vacuum mode. It was interesting to find that the dark bands observed in the low vacuum mode had almost completely lost the microstructural features that distinguished them

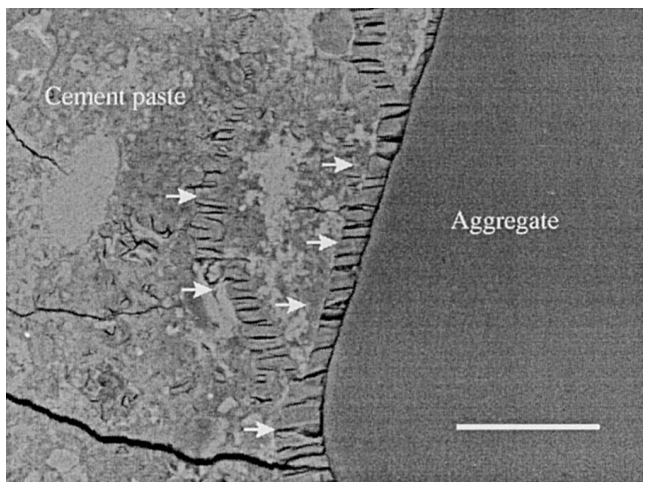

Fig. 1. A bse image of ettringite bands (arrowed) taken by SEM in low vacuum mode. The scale bar indicates the length of 50 μm.

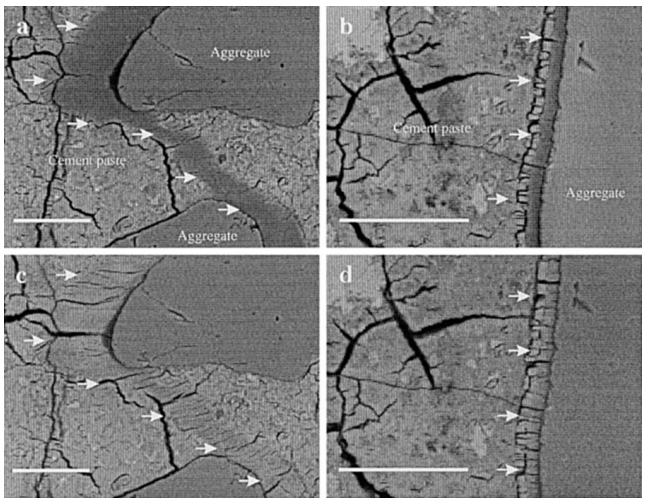

Fig. 2. A bse images of thaumasite bands (arrowed). All the scale bars indicate the length of 50 μm. Micrographs (a) and (b) were taken by SEM in low vacuum mode. Micrographs (c) and (d) were taken by SEM in high vacuum (conventional) mode corresponding to the same fields as micrographs (a) and (b), respectively.

from ettringite. Comparing Fig. 2a and c with Fig. 2b and d, the gray level of the dark bands was turned into the light gray characteristic of ettringite and C-S-H gel, and shrinkage cracks appeared in the bands.

Qualitative X-ray microanalysis was carried out at low vacuum. The dominant elements in the central areas of the dark bands were Ca, Si, and S. Al was more or less present in most of the analyses. A small amount of carbon was detected in the dark bands and also in the cement paste surrounding them. The carbon probably originated from the carbonation of the concrete and the impregnation resin. The composition of the dark *bands* could be attributed to thaumasite, but could also have resulted from C-S-H gel sorbing a certain amount of sulfate [9] or being intermixed with gypsum or ettringite. Quantitative X-ray microanalysis was carried out on the same specimens. The analyses were focused on the material in the dark bands and the ettringite bands. The results are presented in the atomic ratio plots shown in Fig. 3a and b. It should be borne in mind that the analysis volume might partly include the materials around the bands because the bands are narrow. The scattered data spots suggest that the materials analyzed are mixtures. The main groups of analysis spots in the dark bands and the ettringite bands are distributed adjacent to the theoretical atomic ratios of thaumasite and ettringite, respectively, i.e. S/Ca = 1/3, Al/Ca = 0, and Si/Ca = 1/3 for thaumasite and S/Ca = 1/2, Al/Ca = 1/3, and Si/Ca = 0 for ettringite. Almost all the analysis spots fall in or adjacent to the triangle with the atomic ratios of thaumasite, ettringite, and C-S-H gel as the three corners. The composition of C-S-H gel in cement paste is quite variable. Its Si/Ca ranges roughly from 0.5 to 0.7 [12]. S/Ca and Al/Ca of C-S-H gel vary more widely because C-S-H gel sorbs sulfate and intermixes with aluminate bearing hydrates. Accordingly, the corner representing C-S-H gel in Fig. 3 is estimated by extrapolating the data point trends. The above observations suggest that the analyzed materials are primarily mixtures of these three phases. The dominant phase in the dark bands is thaumasite. Thaumasite and ettringite are partially intermixed or in the form of limited solid solutions. Many analyses in the ettringite bands are distributed along the tie line between ettringite and C-S-H gel. This arises from the analysis volumes including the C-S-H gel adjacent to narrow ettringite bands.

Raman spectroscopy gives further confirmation of the presence of thaumasite in the dark bands. Before Raman spectroscopic analysis, the dark bands in the specimens were coordinated in the SEM. Fig. 4 shows the Raman spectrum of the dark band shown in Fig. 2a. The three Raman spectrum peaks, 990, 658, and 460 cm^{-1}, are consistent with the published Raman spectroscopic data for synthetic pure thaumasite with peaks at 993, 663, and 459 cm^{-1} [13]. The peak at 658 cm^{-1} is attributed to the ν_1 frequency of silicon in 6-coordination with oxygen. Thaumasite contains silicon in 6-coordination with hydroxyl ($[Si(OH)_6]^{-2}$) [14–17]. The silicon present in the calcium

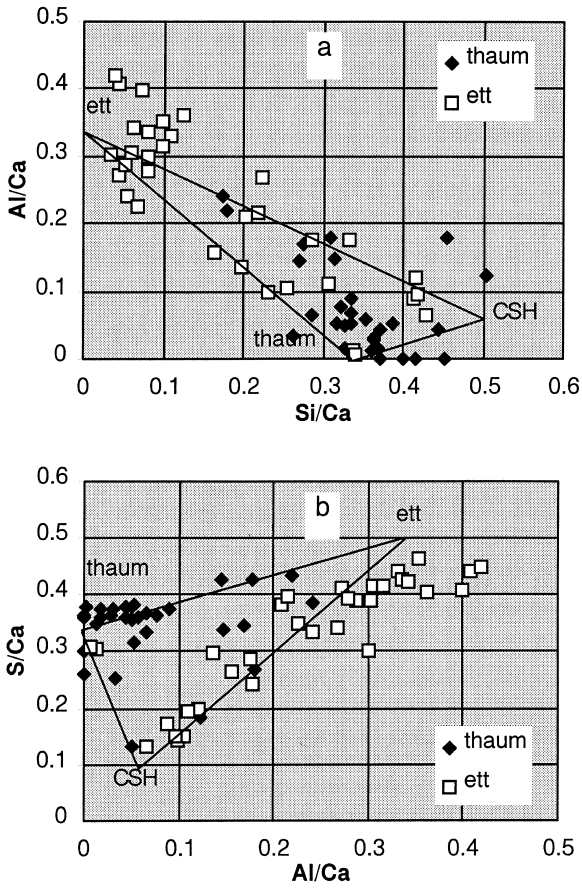

Fig. 3. Quantitative X-ray microanalyses in the thaumasite bands and the ettringite bands expressed in atomic ratios.

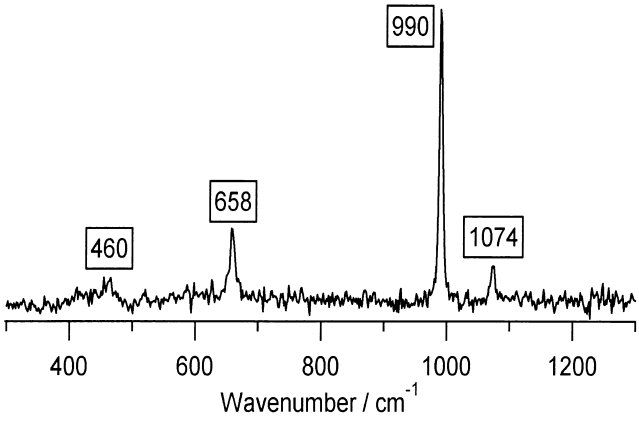

Fig. 4. Raman spectra of the thaumasite band shown in Fig. 2a. The spectrum has been baseline stripped to remove a broad fluorescence background.

silicate hydrates (C-S-H gel) and anhydrous cement (alite and belite) is in tetrahedral coordination with oxygen, which corresponds to a peak in the range 800–1000 cm^{-1}. Therefore, the peak at about 658 cm^{-1} can be regarded as the characteristic band of thaumasite. The peak at 990 cm^{-1} is attributed to the SO_4 ν_1 frequency [13]. The peak at 460 cm^{-1} is unassigned, while that at 1074 cm^{-1} could be due either to SO_4 or CO_3 [10].

The above results confirm that the dark bands observed by bse imaging in the SEM at low vacuum were thaumasite. Differences in water lost by thaumasite and ettringite during drying create differences in the microstructural features of the thaumasite and ettringite bands. Both thaumasite and ettringite shrink on loss of structural water. The shrinkage causes cracking and increases the average atomic number of the material and hence, its bse coefficient and gray scale. The dark thaumasite bands observed under SEM in low vacuum mode show the microstructural features of the thaumasite before losing the majority of its structural water. These observations suggest that thaumasite requires a higher vacuum than ettringite to lose its structural water.

The thaumasite bands were concentrated in isolated areas of the cement paste and the paste–aggregate transition zone. Some of them passed through the siliceous aggregate particles. The aggregate was very low in carbonate. The source of carbonate for thaumasite formation was probably calcite due to carbonation of the cement paste or carbonate ions in the ground water. The amount of thaumasite formed was significantly less than that of ettringite.

4. Conclusions

- In high vacuum bse images of concrete blocks dried at 50°C and resin impregnated, thaumasite and ettringite bands appear heavily cracked and of similar gray scale. They can be differentiated by X-ray microanalysis, but this is laborious and sometimes imprecise.
- In low vacuum bse images of the same specimens (prior to exposure to a high vacuum), the appearance of ettringite is similar to that in high vacuum, but thaumasite is different, with very few cracks and a darker gray scale.
- Therefore, low vacuum SEM can be used to identify thaumasite and to differentiate between thaumasite and ettringite. The technique has the potential to play an important role in diagnosing the type and extent of sulfate attack of site concrete and in investigating sulfate attack mechanisms.

Acknowledgments

The authors acknowledge Dr. Adrian Brough and Prof. Alan Atkinson (Department of Materials, Imperial College of Science, Technology and Medicine) for undertaking the Raman spectroscopic measurements. We are also grateful to Dr. Karen Scrivener (Laboratoire Central de Recherche, Lafarge) and Dr. Norah Crammond (Building Research Establishment, UK) for helpful discussions.

References

[1] N.J. Crammond, Thaumasite in failed cement mortars and renders from exposed brickwork, Cem Concr Res 15 (1985) 1039–1050.
[2] U. Ludwig, S. Mehr, Destruction of historical buildings by the formation of ettringite or thaumasite, 8th Inter Cong Cem Chem Rio 5, (1986) 181–188.
[3] G. Baronio, M. Berra, Concrete deterioration with the formation of thaumasite — analysis of the causes, Cemento part 3 83 (1986) 169–184.
[4] J.A. Bickley, R.T. Hemmings, R.D. Hooton, J. Balinski, Thaumasite related deterioration of concrete structures, Conference of Concrete Technology, Past, Present and Future, San Francisco: ACI SP 144-8 (1995) 159–178.
[5] N.J. Crammond, M.A. Halliwell, The thaumasite form of sulfate attack in concretes containing a source of carbonate ions — a microstructural overview, advances in concrete technology, Proceedings: Second CANMET/ACI International Symposium, Las Vegas, Nevada, USA, (1995) 357–380.
[6] Report of the thaumasite expert group, The thaumasite form of sulfate attack: Risks, diagnosis, remedial works, and guidance on new construction, Department of the Environment, Transport and the Regions, London, 1999.
[7] C. Rogers, M. Thomas, H. Lohse, Thaumasite from Manitoba and Ontario, 19th International Conference on Cement Microscopy, Cincinatti, USA (1997) 306–319.
[8] N.J. Crammond, Quantitative X-ray diffraction analysis of ettringite, thaumasite and gypsum in concretes and mortars, Cem Concr Res 15 (1985) 431–441.
[9] I. Odler, Investigation between gypsum and the C-S-H gel formed in C_3S hydration, 7th International Congress on Chemistry of Cement, Paris IV, (1980) 496–503.
[10] A.R. Brough, A. Atkinson, Micro-Raman spectroscopy of thaumasite — a diagnostic tool, Cem Concr Res, in preparation.

[11] R. Yang, C.D. Lawrence, J.H. Sharp, Delayed ettringite formation in 4-year old cement pastes, Cem Concr Res 26 (1996) 1649–1659.
[12] H.F.W. Taylor, Cement Chemistry, Academic Press, London, 1990.
[13] J. Bensted, S. Prakash Varma, Studies of thaumasite — Part II, Silic Ind 1 (1974) 11–19.
[14] H. Moenke, Ein weiteres mineral mit silizium in 6er-koordination: Thaumasite, Naturwissenschaften 51 (1964) 239.
[15] R.A. Edge, H.F.W. Taylor, Crystal structure of thaumasite, a mineral containing[$Si(OH)_6$]$^{-2}$-groups, Nature (London) 224 (1969) 363–364.
[16] A. Laffaille, J. Protas, Nouvelles données sur la structure de la thaumasite, Comptes rendus hebdomadaires des Séances de l'Académie des Sciences Paris, Série D 270, (1970) 2151–2154.
[17] J. Skibsted, L. Hjorth, H.J. Jakobsen, Quantification of thaumasite in cementitious materials by 29Si and 1H cross-polarization magic-angle spinning NMR spectroscopy, Adv Cem Res 7 (1995) 69–83.